Slotted-Wall Blockage Corrections for Disks and Parachutes

J. Michael Macha,* Robert J. Buffington,† and John F. Henfling‡
Sandia National Laboratories, Albuquerque, New Mexico 87185
and
David Van Every§ and John L. Harris¶
DSMA International, Inc., Mississauga, Ontario L4V 1V8, Canada

Bluff shapes, including parachutes, often require large blockage corrections when tested in solid-wall wind tunnels. The magnitude of the correction is much smaller in test sections with slotted walls, but the blockage becomes a complicated function of model size, wall porosity, and upstream and downstream boundary conditions. Disk and parachute models were tested in a low-speed wind tunnel where the slotted-wall open area ratio and model axial position were systematically varied. In steady flow, the benefit of the wall slots was achieved asymptotically as the models were moved downstream from the leading edge of the slots, and this flow development length increased with decreasing wall porosity and increasing model size. The experiments with the parachutes provided the first quantitative information on wall interference and tunnel circuit response during the nonsteady inflation process. There was no observable blockage effect during the inflations with any of the slotted-wall configurations studied.

Nomenclature

A = tunnel cross-sectional area
C_D = drag coefficient in steady flow
$C_{\hat{D}}$ = peak value of C_D for an inflating parachute
q = test section dynamic pressure
S = model frontal projected area
S_c = constructed area of a parachute canopy
x = model axial position
δ_f = diffuser flap setting

Subscript

∞ = free of wall interference

Introduction

BLUFF bodies, in general, and parachutes, in particular, often require large blockage corrections when tested in conventional solid-wall wind tunnels. The semiempirical correction method developed by Maskell[1] has been successfully applied to a variety of rigid shapes whose aerodynamics is dominated by a region of separated flow. In a recent experimental study,[2] this method was extended to flexible, cloth parachutes of standard design under steady-flow conditions. Typically, the uncorrected drag coefficient of a parachute presenting a geometric blockage of 10% (i.e., $S/A = 0.1$) in a solid-wall test section can be in error by up to 30%. The relatively large dimensional tolerances associated with fabric construction and the requirement to replicate elastic properties place a practical limit on the miniaturization of model parachutes. As a result, it is often impossible to observe even a modest upper limit on geometric blockage, except in very large wind tunnels.

Received May 26, 1990; presented as Paper 90-1407 at the AIAA 16th Aerodynamic Ground Testing Conference, Seattle, WA, June 18-20, 1990; revision received Oct. 16, 1990; accepted for publication Oct. 25, 1990.

*Senior Member of Technical Staff, Parachute Systems Division. Associate Fellow AIAA.
†Senior Member of Technical Staff, Experimental Aerodynamics Division. Member AIAA.
‡Senior Technical Aide, Experimental Aerodynamics Division.
§Intermediate Aerodynamicist.
¶Senior Aerodynamicist.

While Maskell's method was shown to accurately correct parachute drag and base-pressure coefficients at geometric blockages as high as 22%, there are occasions when it is desirable to reduce the severity of test-section boundary effects. One example is the measurement of the pressure distribution over both the attached- and separated-flow regions of the canopy. Because the wall-induced interference velocity varies over the length of a model, local pressure coefficients require corrections based on local flow conditions if the boundary effect is large. Maskell's method provides only an average correction to the flow in the vicinity of the model. Furthermore, the empirical factor derived in Ref. 2 for the Maskell equation may not be appropriate for all types of parachutes. If parachutes could be tested under boundary-constraint conditions less severe than those imposed by solid walls, the resulting smaller correction would demand less accuracy from whatever correction method was used.

The possibility of using ventilated walls to minimize boundary interference derives from the earliest theoretical studies comparing solid-wall to open-jet test sections. Many of the interference effects are of opposite sign for these two extreme geometries; hence, by using a partially open tunnel, it is possible to reduce, or even eliminate, some aspects of boundary interference. Reference 3 gives a comprehensive summary of the theoretical treatment of subsonic wall interference for both slotted and perforated walls. The subsequent development of transonic test sections using ventilated walls for both Mach number control and shock wave cancellation has continued to encourage the pursuit of a general theory of the ventilated-wall boundary condition.[4,5]

Past studies of slotted-wall blockage have dealt almost exclusively with streamlined shapes because they represent the bulk of testing activity. An exception is the experimental and analytical investigation of boundary corrections for models of semibluff road vehicles reported in Ref. 6. Since a truly bluff shape is inherently more difficult to analyze even in the absence of tunnel walls, practical information about the effects of slotted walls on the measured aerodynamic characteristics of parachutes can be obtained only by experimentation. For conventional parachutes with axial symmetry, lift interference is usually not a factor; only the blockage interference, which stems from the velocity increment and gradient in the vicinity of the model, need be considered. Although most parachute testing in wind tunnels consists of steady-flow measurements on models of fixed geometry, it is sometimes

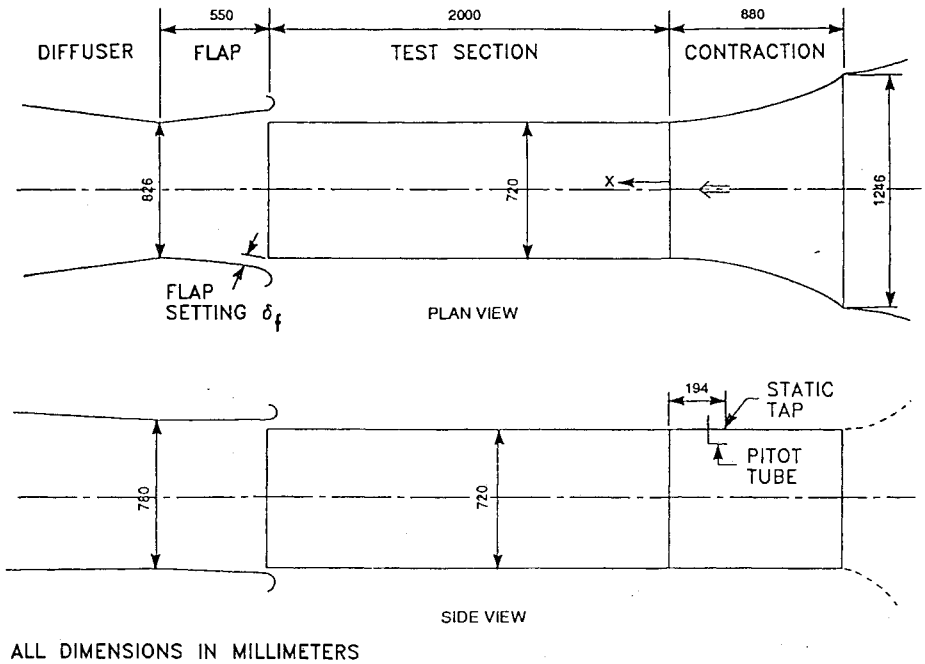

Fig. 1 Sketch of the DSMA 0.72- × 0.72- × 2-m-long test section.

necessary to measure time-dependent forces and pressures as a parachute inflates.[7,8] During inflation, the projected area of the model changes rapidly and the instantaneous drag reaches a peak that may be twice the fully inflated, steady-flow value because of the effect of the added mass of air. The nature of wall interference during the inflation process has not been previously addressed in the literature.

This paper presents the results of an experimental study of low-speed, slotted-wall blockage for bluff bodies, with emphasis on parachutes. Fundamental new information about the effects of model axial position and wall porosity on steady-flow blockage was obtained using rigid disk models. Additional measurements with model parachutes provide, for the first time, quantitative data on solid- and slotted-wall blockage during the nonsteady, inflation process. Changes in total and dynamic pressure caused by the rapidly increasing drag of an inflating parachute are also presented and discussed. The study gives guidance for the optimum use of slotted-wall wind tunnels when testing parachutes or other bluff objects.

Experimental Apparatus and Procedure

Wind Tunnels

The experiments were done primarily in the closed-circuit DSMA wind tunnel with the 0.72- × 0.72- × 2-m-long test section shown in Fig. 1. The adjustable flaps at the mouth of the diffuser formed the flow re-entry section required for the slotted-wall configurations. In the solid-wall configuration, the flaps were opened a small amount to serve as the test-section breather. Nominal wall open area ratios (OAR) of 0, 0.1, 0.2, and 0.3 were achieved by fitting panels of appropriate width to a framework around the test section. Figure 2 shows the details of the wall geometry, including the actual as-built porosities. In this paper, the nominal OARs are used to identify the different wall configurations. The test section had corner fillets designed to compensate for the growth of the wall boundary layer on the solid walls. The fillets remained installed with the slotted walls. The test section was surrounded by an infinite-volume plenum consisting of the high-bay room housing the wind-tunnel circuit.

It was anticipated that the loss of flow energy associated with the sudden increase in drag of an inflating parachute would decrease the velocity in the tunnel circuit. Such a decrease would tend to obscure the true, blockage-induced change in velocity in the vicinity of the model. To minimize

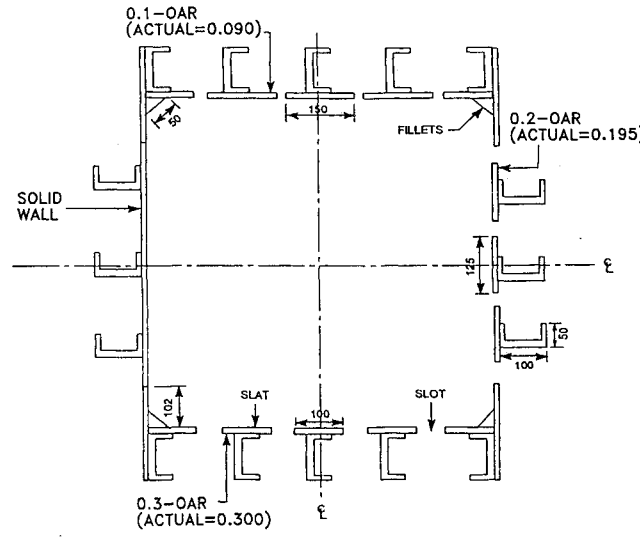

Fig. 2 Sectional view of the DSMA test section at axial station $x/\sqrt{A} = 1.39$. (Composite of the four wall configurations tested.)

this contamination of the wall-interference data, a set of fabric and wire screens was added upstream of the fan section to increase circuit losses and make the effect of the model less apparent. In quantitative terms, the overall loss of total pressure around the circuit, as a fraction of test section dynamic pressure, was increased from 0.56 to 3.29.

Prior to the experiments in the DSMA facility, all of the models were tested in the much larger 16- × 23-ft test section of the Lockheed-Georgia wind tunnel. With a maximum geometric blockage of only 0.0025, these initial tests provided baseline data that were essentially free of wall interference and changes in freestream velocity.

Models

The four disk models had geometric blockage ratios (S/A) in the DSMA wind tunnel of 0.02, 0.05, 0.10, and 0.15. Actual diameters are listed in Table. 1. All disks were 0.125 in. thick, with a rearward-facing, 45-deg chamfer around the periphery. The three parachute models were of flat, circular design with

Table 1 Reference data for the disk models

Diameter, in.	S/A	$C_{D\infty}$
4.52	0.020	1.168
7.15	0.050	1.166
10.11	0.100	1.161
12.39	0.150	1.158

Table 2 Reference data for the parachute models

Constructed diameter, in.	Approximate S/A	$C_{D\infty}$	$C_{\hat{D}\infty}$
10.0	0.05	0.590	1.118
14.5	0.10	0.580	1.020
18.0	0.15	0.591	1.115

constructed diameters of 10.0, 14.5, and 18.0 in. The canopies were fabricated from a lightweight (1.1 oz/yd^2), impermeable nylon cloth and were perforated with 0.375-in.-diam holes to provide a geometric porosity of approximately 15%. Each model had 12 suspension lines made from 60-lb-breaking-strength Kevlar thread, with length equal to the constructed diameter. The inflated diameters were approximately 70% of the constructed diameters, giving values of S/A approximately the same as for the three largest disk models. The reference data for the parachute models are summarized in Table 2.

The models were supported in the test section using a conventional sting and strut arrangement. The sting, which contained an integral strain-gauge balance to measure the aerodynamic loads on the models, could be translated in the strut to permit the models to be positioned at any axial station. With the parachutes, the sting passed through the center vent of the canopy and the ends of the suspension lines were captured in a special nose piece attached to the front of the sting. The same sting was used with a taller strut in the Lockheed-Georgia wind tunnel.

Test Procedure

Airflow conditions in the DSMA test section were determined from measurements of total and dynamic pressure near the exit of the contraction section. The pitot tube and wall orifice, whose locations are indicated in Fig. 1, were close coupled to a pair of low-volume pressure transducers. This arrangement was necessary to measure the rapidly changing conditions during the inflation of the parachute models. A simple but reliable method was used to initiate the inflations. Before starting the tunnel, a lightweight line was tied tightly around the suspension lines and sting just upstream of the parachute's skirt and routed back to the strut and down to a weight suspended below the test section. With the desired flow conditions established, the suspended weight was released, thus undoing the slip knot and allowing the parachute to inflate.

Airspeed in the DSMA wind tunnel was adjusted to give the same steady-flow drag force that had been measured at the Lockheed-Georgia facility. This approach insured that all measurements for a given model were made at the same corrected dynamic pressure, regardless of the wall configuration. As a result, there were no variations in Reynolds number and, in the case of the elastic parachutes, no variations in inflated shape that could obscure the wall-interference effects. The nominal corrected dynamic pressure was 10 psf, yielding corrected Reynolds numbers based on model projected diameter in the range 2.4×10^5–6.5×10^5.

Measurement Accuracy

The absolute accuracies of the measurements were determined to be ± 0.1 psf for pressures and ± 0.05 lb for model drag. The propagation of uncertainties in the calculation of the drag coefficient from these measurements was estimated using the method of Kline and McClintock (see, e.g., Ref. 9). For the smallest disk model (i.e., $S/A = 0.02$), the worst case uncertainty was $\pm 2\%$; for the largest disk and parachute models ($S/A = 0.15$), the uncertainty was less than $\pm 1\%$.

Discussion of Experimental Results

Model Location and Diffuser Flap Setting

Before presenting specific test results, it is instructive to summarize the observed effects of model axial position on slotted-wall blockage. A model located at the start of the test section experienced a solid-wall type of blockage with the measured C_D too large. As the model was moved downstream, outflow through the slots ahead of the model relaxed the wall constraint and the uncorrected C_D decreased. If the test section was long enough for a particular size model, a region was reached where the slot flow was fully developed and C_D was independent of positon. Model size and wall porosity together determined the distance required to establish this constant-blockage region. With the model downstream from the constant-blockage region and approaching the end of the test section, there was no longer sufficient slot length behind the model to allow inflow without incurring a streamwise static pressure gradient. The geometry at the mouth of the diffuser strongly influenced the nature of the pressure gradient, as discussed in the following.

With slotted walls, the portion of the flow displaced by the model wake remained outside of the test section. Some means had to be used to direct this fluid into the diffuser while minimizing the streamwise static pressure gradient in the test section. In the present tests, the re-entry section consisted of an adjustable flap on each of the four walls at the mouth of the diffuser, as shown in Fig. 1. If the flap setting δ_f was too small for a given size model and wake, a negative pressure gradient existed in the aft portion of the test section; conversely, if δ_f was too large, a positive pressure gradient occurred. In either case, an appropriate buoyancy correction would be required (in addition to the blockage correction) if the model was located too near the end of the test section. This complication was avoided only by restricting model placement to locations upstream of the region of re-entry flap influence. Consequently, a flagrantly incorrect flap setting would severely shorten the usable length of the test section.

Disk Blockage

Drag coefficients for the disk models measured in the Lockheed-Georgia wind tunnel and corrected for the nearly negligible, solid-wall blockage using the method of Maskell[1] are listed in Table 1 under the heading $C_{D\infty}$. Although the variation in $C_{D\infty}$ among the four models is nominally within the estimated measurement uncertainty, it may include slight influences of Reynolds number and the interference from the constant-diameter sting support.

For each slotted-wall OAR in the DSMA wind tunnel, the sensitivity of C_D to model axial location and the setting of the

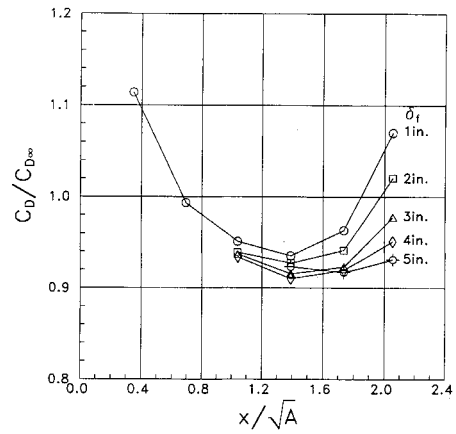

Fig. 3 Effect of re-entry flap setting for the $S/A = 0.1$ disk with the 0.3-OAR wall configuration.

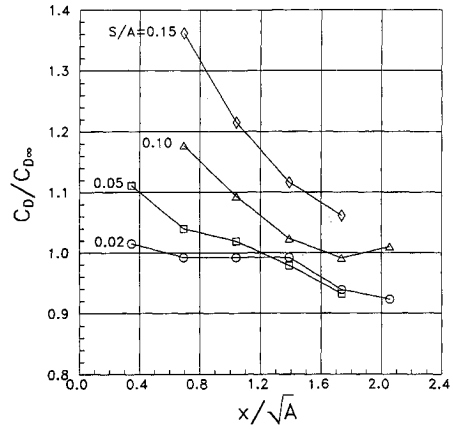

Fig. 4 Disk blockage correction as a function of model size and axial location for the 0.1-OAR wall configuration.

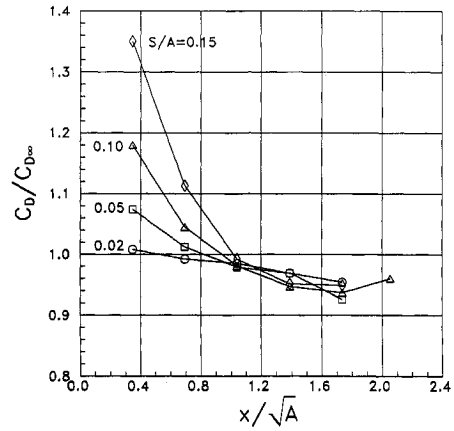

Fig. 5 Disk blockage correction as a function of model size and axial location for the 0.2-OAR wall configuration.

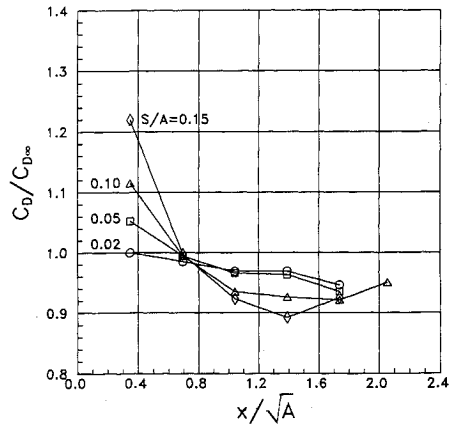

Fig. 6 Disk blockage correction as a function of model size and axial location for the 0.3-OAR wall configuration.

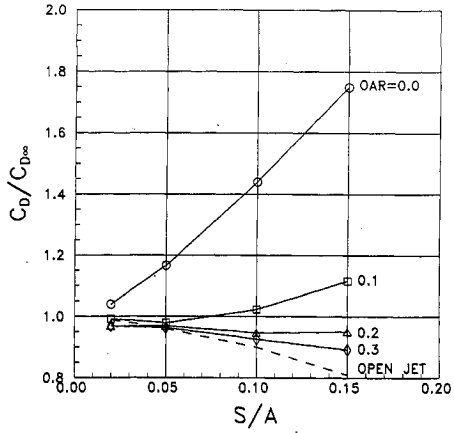

Fig. 7 Disk blockage correction at the center of the test section as a function of geometric blockage ratio and wall OAR.

diffuser re-entry flaps was determined using the $S/A = 0.1$ disk. Results for the 0.3-OAR wall are shown in Fig. 3. The blockage correction (i.e., the measured C_D normalized by $C_{D\infty}$ for that model) is plotted as a function of nondimensional distance from the upstream end of the test section $x/\sqrt{A}$ and flap setting δ_f. The downstream end of the test section is at $x/\sqrt{A} = 2.78$. The curve illustrates that the negative pressure gradient associated with the smallest flap setting of 1 in. caused a significant increase in C_D as far forward as the middle of the test section. On the other hand, C_D was insensitive to flap position for 3 in. $\leq \delta_f \leq 5$ in. as far aft as $x/\sqrt{A} = 1.73$. Based on these data and additional results for the 0.1- and 0.2-OAR walls, it was determined that $\delta_f = 4$ in. was a near-optimum setting for all of the disk and parachute models, and $x/\sqrt{A} = 1.39$ (i.e., the center of the test section) was the aftmost model location for measurements to be reasonably unaffected by the downstream termination of the slots.

Figures 4-6 present the variation of disk blockage correction as a function of axial position and model size for each of the three slotted-wall configurations, with $\delta_f = 4$ in. Comparing these figures shows that the slot-flow development distance increased as the wall OAR decreased for a given size model. This trend is especially apparent for the two largest disks. It is also clear from the figures that the development distance increased with increasing model size. In the case of the 0.1-OAR wall, the test section was sufficiently long to achieve the full benefit of the slots for only the smallest disk. With the 0.2-OAR wall, asymptotic values of C_D were achieved for both the $S/A = 0.02$ and 0.05 disks. With the 0.3-OAR wall, the test section was long enough for all but the largest disk.

The variation of disk blockage correction with model size and wall OAR at the middle of the test section is summarized in Fig. 7. The data for the solid-wall configuration are in excellent agreement with previous measurements using disks reported in Ref. 10. Consistent with other analyses and experiments reported in the literature for more streamlined shapes, the interference effect on C_D is opposite in sign for the solid and slotted walls. Moreover, the magnitude of the required correction is smaller by a factor of at least 5 for the slotted walls. The dashed curve in Fig. 7 is an approximate, theoretical correction for an open-jet test section of the same dimensions. The open-jet values were determined from the measured interference with solid walls and the theoretical relationship between closed and open test sections presented in Ref. 3. If the test section had been long enough to allow full development of the slotted-wall flow for all of the OARs and model sizes tested, the variation of C_D with increasing geometric blockage would follow the trend exhibited by the open-jet curve.

Parachute Blockage

Steady-flow drag was measured at the end of each of the parachute inflation tests. Reference values of $C_{D\infty}$ obtained in the Lockheed-Georgia wind tunnel and corrected for the very slight blockage using the method suggested in Ref. 2 are listed in Table 2. Drag coefficients for the parachute models are based on the constructed area of the canopy S_c.

All parachute testing in the DSMA wind tunnel was done with the skirt of the inflated canopy located at the center of the test section, $x/\sqrt{A} = 1.39$. During those tests, it was observed that the inflated shape of the 14.5-in.-diam parachute was changing. Close examination showed that the skirt of the canopy was sliding up some of the suspension lines toward the vent, thereby decreasing the projected area. The reduction in inflated size was confirmed by the fact that the measured drag coefficient in the presence of the solid wall was

approximately 6% lower than expected based on $C_{D\infty}$ and the blockage correction method of Ref. 2. Consequently, comparisons between the DSMA and Lockheed-Georgia data for this model were excluded from the analysis. The steady-flow drag data obtained in the DSMA wind tunnel for the other two parachute models are summarized in Fig. 8. Since the frontal projected areas of the inflated parachutes are not precisely known, the geometric blockage ratio has been replaced by an aerodynamic blockage ratio based on the interference-free drag area, $(C_{D\infty}S_c)/A$. As expected, the steady-flow parachute data show the same trend with OAR as observed for the disk data.

Even with the additional pressure-drop screens installed in the DSMA tunnel, a measurable decrease in test-section velocity occurred as the parachutes inflated. Within measurement accuracy, the decrease was independent of wall OAR for the two smaller models. Specifically, for geometric blockage ratios of 0.05 and 0.10, the average losses in freestream dynamic pressure were 1.2% and 2.9%, respectively. For the largest model ($S/A = 0.15$), the drop in dynamic pressure decreased slightly from 6.4 to 4.9% as the wall OAR increased from 0.0 to 0.3. The dynamic aspects of these changes in test-section conditions during the inflation event are discussed in the following paragraphs.

Figure 9 displays the direct instrument outputs for the largest parachute ($S/A = 0.15$) inflating in the presence of the solid walls. The decrease in test section dynamic pressure occurred simultaneously with the increase in model drag. At the instant when the peak drag was reached, the dynamic pressure had realized approximately one-half of its eventual decrease. The lowest trace shows that test-section total pressure increased during the inflation, and examination of the reduced data indicates that a significant increase in static pressure of $\Delta p_s/q = 0.33$ occurred. Since this change in static pressure could not have occurred simultaneously over the length of the test section, it must be assumed that the measured drag of the model was affected to some unknown degree by a time-varying, horizontal buoyancy force. Figure 10 presents results for the same model, but with the 0.2-OAR slotted walls. The significant effect of the ventilated test section was to delay the changes in total and dynamic pressure until after the parachute had completely inflated. Consequently, drag measurements during inflation with the slotted walls were not subject to the buoyancy force present with the solid walls. The eventual decrease in total pressure shown in Fig. 10 is consistent with the constant static-pressure environment provided by the surrounding plenum.

A quantitative assessment of the influence of the test-section walls on the inflation event can be made by examining the peak drag as a function of wall OAR for each of the model sizes. In Fig. 11, the peak value of the drag coefficient $C_{\hat{D}}$ normalized by the peak interference-free value $C_{\hat{D}\infty}$ (measured in the Lockheed-Georgia wind tunnel) is plotted as a function of the steady-flow aerodynamic blockage ratio and wall OAR. Each of the symbols in the figure represents an average of several repeated inflations. The scatter in the data for a given model and wall configuration caused by the random nature of the inflation process was approximately ±6%.

The solid-wall data in Fig. 11 marginally suggest a positive correlation between model size and $C_{\hat{D}}$. Comparing this result to the large solid-wall blockage for the steady-flow condition (recall Fig. 8) suggests that a finite time, greater than the approximately 100 ms taken to reach peak drag, was required for the full effect of the walls to be felt by the model. However, it must be kept in mind that $C_{\hat{D}}$ is based on the dynamic pressure that existed at the start of the inflation; it may be appropriate to adjust the coefficient upward by a few percent to account for the subsequent decrease in dynamic pressure depicted in Fig. 9. Even so, the true solid-wall blockage would remain inseparable from the undetermined, nonsteady buoyancy force.

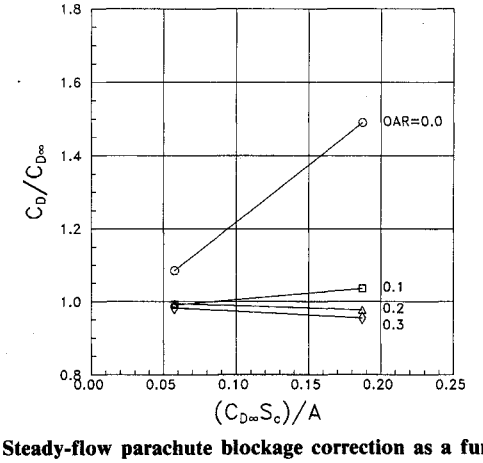

Fig. 8 Steady-flow parachute blockage correction as a function of aerodynamic blockage ratio and wall OAR.

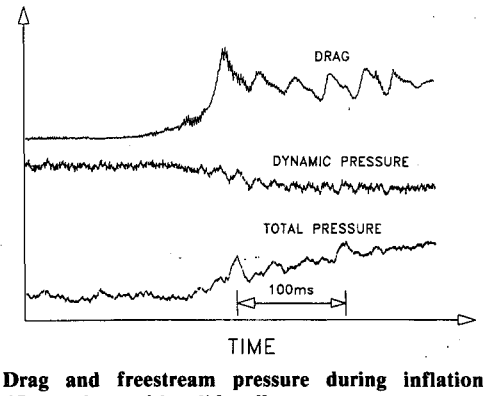

Fig. 9 Drag and freestream pressure during inflation of the $S/A = 0.15$ parachute with solid walls.

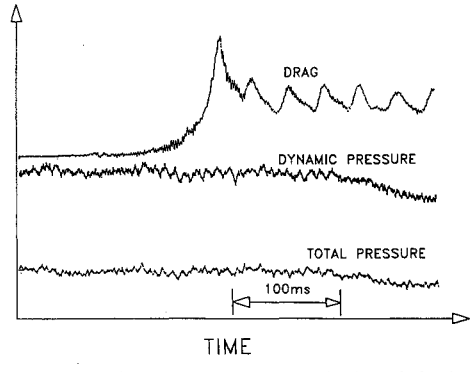

Fig. 10 Drag and freestream pressure during inflation of the $S/A = 0.15$ parachute with the 0.2-OAR slotted walls.

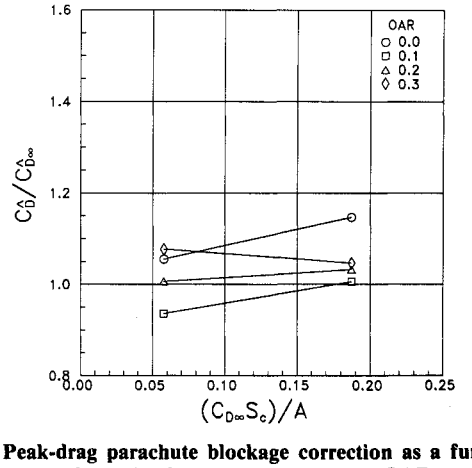

Fig. 11 Peak-drag parachute blockage correction as a function of steady-flow aerodynamic blockage ratio and wall OAR.

In the case of the slotted-wall data presented in Fig. 11, the values of $C_{\hat{D}}$ are subject to neither a decrease in dynamic pressure nor the complication of a buoyancy force. Within the scatter inherent in the random nature of the inflations, there was no detectable blockage effect on $C_{\hat{D}}$ for any of the slotted-wall configurations.

Summary and Conclusions

An experimental study of slotted-wall blockage was performed using disk and parachute models in a low-speed wind tunnel. Test-section open area ratio, model geometric blockage ratio, and model location along the length of the test section were systematically varied. Resulting drag coefficients were compared to each other and to interference-free measurements obtained in a much larger wind tunnel where the geometric blockage ratio was less than 0.0025.

The steady-flow disk data provide new insight into the nature of slotted-wall interference for axisymmetric or other low aspect ratio bluff shapes. Specifically, the test results support the following conclusions.

1) The geometry of the displaced-flow re-entry device at the downstream end of the test section could significantly influence model drag as far forward as the middle of the test section, depending on model size and wall OAR.

2) The full benefit of the slots was achieved asymptotically as the model was moved downstream from the leading edge of the slots, and this development length increased with decreasing wall OAR and increasing model size.

3) The interference effect on drag coefficient was opposite in sign for the slotted and solid walls, and the magnitude of the required correction was smaller by a factor of at least five with the slotted walls.

The experiments with the parachute models have provided the first quantitative information on tunnel circuit response and wall interference during the inflation process. The following additional conclusions pertain to these dynamic effects.

4) In the case of the solid walls, dynamic pressure decreased and static pressure increased during inflation. It is conjectured that the pressure change at the measurement location was accompanied by a nonsteady static-pressure gradient in the test section, producing a horizontal buoyancy force of undetermined strength.

5) With the slotted walls, the decrease in dynamic pressure occurred after the parachute was completely inflated. A concurrent decrease in total pressure confirmed that the static pressure in the test section remained constant and equal to the pressure in the surrounding plenum.

6) The time-dependent drag data with the solid walls marginally suggest an increase in peak drag coefficient with increasing blockage ratio. The observed increase in $C_{\hat{D}}$ was the result of the combined effects of conventional solid-wall blockage (albeit, with an undetermined time lag), the decrease in velocity caused by increased energy loss in the circuit, and the nonsteady static-pressure gradient within the test section.

7) Within measurement accuracy and subject to the random nature of the inflation process, there was no discernible wall-interference effect on $C_{\hat{D}}$ for any of the slotted-wall configurations.

Acknowledgments

This work was supported in part by the U. S. Department of Energy under Contract DE-AC04-76DP00789. The authors thank Dave Powers of Sandia National Laboratories for his help in obtaining the reference model data at the Lockheed-Georgia wind tunnel.

References

[1]Maskell, E. C., "A Theory of the Blockage Effects on Bluff Bodies and Stalled Wings in a Closed Wind Tunnel," Royal Aircraft Establishment, London, Rept. 2685, Nov. 1963.

[2]Macha, J. M., and Buffington, R. J., "Wall-Interference Corrections for Parachutes in a Closed Wind Tunnel," *Journal of Aircraft*, Vol. 27, No. 4, 1990, pp. 320–325.

[3]Rogers, E. W. E., "Wall Interference in Tunnels with Ventilated Walls," *Subsonic Wind Tunnel Wall Corrections*, NATO, Paris, AGARDograph 109, Oct. 1966, Chap. 6.

[4]Barnwell, R. W., "Improvements in the Slotted-Wall Boundary Condition," *Proceedings of the 9th Aerodynamic Testing Conference*, AIAA, New York, 1976, pp. 21–30.

[5]Everhart, J. L., "Theoretical and Experimental Analysis of the Slotted-Wall Flow Field in a Transonic Wind Tunnel," Society of Automotive Engineers, Warrendale, PA, Paper 871757, Oct. 1987.

[6]Templin, J. T., and Raimondo, S., "Experimental Evaluation of Test Section Boundary Interference Effects in Road Vehicle Tests in Wind Tunnels," *Journal of Wind Engineering and Industrial Aerodynamics*, Vol. 22, 1986, pp. 129–148.

[7]Croll, R. H., Klimas, P. C., Tate, R. E., and Wolf, D. F., "Summary of Parachute Wind Tunnel Testing Methods at Sandia National Laboratories," AIAA Paper 81-1931, Oct. 1981.

[8]Klimas, P. C., "Inflating Parachute Canopy Differential Pressures," *Journal of Aircraft*, Vol. 16, No. 12, 1979, pp. 861,862.

[9]Holman, J. P., and Gajda, W. J., *Experimental Methods for Engineers*, 4th ed., McGraw-Hill, New York, 1984, Chap. 3.

[10]Holst, H., "Wind Tunnel Wall Interference in Closed, Ventilated and Adaptive Test Sections," *Wind Tunnel Wall Interference Assessment and Correction*, NASA CP-2319, 1984, pp. 61–78.